Revista Colombiana de Física, Vol. 42, No. 3 de 2010.

Vibrational Raman Modes Relating to Mn_mAs_n clusters

Modos Raman Vibracionales de cluster Mn_mAs_n

A. Pulzara Mora [*a], M. López Lopez [b], y A. Rosales Rivera [a]

[a] *Laboratorio de Magnetismo y Materiales Avanzados, Universidad Nacional de Colombia, sede Manizales. A. A. 127.*
[b] *Centro de Investigación y Estudios Avanzados del IPN, México 07000, Distrito Federal, México*

Recibido 19.04.10; Aceptado 07.12.10; Publicado en línea 17.04.11.

Resumen

En este trabajo reportamos los modos Raman vibracionales de cluster de Mn_mAs_n, formados en aleaciones semimagnéticas de GaAsMn. Debido a las altas temperaturas de deposición (400 oC <Tg<500 oC), las muestras de GaAsMn son muy ricas en Mn, promoviendo la formación de enlaces de Mn-As. Para estimar teóricamente las frecuencias de vibración de los modos fonónicos relacionados a los clusters de Mn_mAs_n, utilizamos el modelo de masa reducida. Los valores calculados teóricamente están en muy buen acuerdo con los valores experimentales obtenidos de los espectros Raman. Las propiedades estructurales y ópticas de las películas mostraron ser muy sensibles a defectos estructurales, tales como aglomeraciones aleatorias de Mn (Mn_{Randon}) que promueven la formación de aglomerados de Mn_mAs_n.

Palabras clave: Espectrosocopia Raman; Cluster de MnAs.

Abstract

In this work, we report the vibrational Raman modes relating to Mn_mAs_k, formed on semimagnetic alloys of GaAsMn. Due to high growth temperatures (400 ^oC <Tg<500 ^oC), the samples are very Mn rich, which promoted Mn atoms forming Mn-As bond. The theoretical calculations by using the reduced mass model are in good agreement with the experimental data obtained from Raman spectra. The optical and structural properties of the GaAsMn showed to be very sensible to structural defects such as random Mn clusters, and promoting the Mn_mAs_n cluster formation.

Keywords: Raman spectroscopy; MnAs clusters.

PACS: 82.80.Gk; 61.46.Bc.

1. Introducción

The development of a novel class of materials combining standard semiconductors with magnetic elements has recently been driven by considerable technological as well as fundamental scientific interest. Among the different possibilities to elaborate ferromagnetic (FM) semiconductors, the incorporation of manganese in a GaAs matrix is one of the most promising ones. Most of the current studies deal with (Ga,Mn)As diluted phases grown by molecular beam epitaxy [1]. This class of materials displays Curie temperatures (T_C) in the range of 80–170 K, and this severely limits their potential application [2,3]. Very recently, a higher T_C has been reported in the stoichiometric MnAs phase, and MnAs nanoclusters (ncs) buried in GaAs fabricated by using MBE followed by annealing [4]. In this system, the nanoclusters of GaMn and MnAs are strongly correlated with the Curie temperature. On the other hand, it is well known that both GaMn and MnAs clusters present room temperature ferromagnetism [5]. It is also known that

* aopulsaram@unal.edu.co

increasing the substrate temperature (Ts) leads to an enhancement of the phase segregation process or of the MnAs clusters concentration in the GaMnAs matrix [6]. The phase separation process or precipitation of MnAs clusters in GaMnAs matrix was observed when Mn content is more than 5% [7].

In this work, we study the formation of MnAs cluster and the influence on structural and optical properties of $Ga_{1-x}Mn_xAs$ thin films grown by using RF magnetron sputtering technique. The samples were characterized by X-Ray diffraction, scanning electron microscopy (SEM), energy dispersive spectroscopy (EDS), atomic force microscopy (AFM), and Raman spectroscopy, in order to determine their structural characteristics, chemical composition, surface morphology, crystal structure and optical properties of the samples.

2. Experimental Details

$Ga_{1-x}Mn_xAs$ films were grown by RF planar magnetron sputtering using as targets a (100) oriented GaAs wafer and a Mn disc. The sputtering system has two cooled targets of 1 inch diameter each one, and controlled independently by RF sources. The growth temperature (Tg) was monitored using a thermocouple embedded in the substrate holder. No substrate bias was used and the base pressure was of $1.2x10^{-6}$ Torr. The flow rate gas was controlled by using a needle valve.

The films were deposited on (100) GaAs substrates located at 5 cm. between targets and the holder substrate. The substrates were cleaned by using standard methods. Before deposition the working pressure was held constant at $1.2x10^{-2}$ Torr and the plasma between target and main shutter was initiated using Argon gas with 99.9% purity. Then the main shutter was opened to start the deposition for a fixed time of 1 h. The growth temperature was varied from 400 to 520 ^oC. Finally, after the film deposition, RF power and gas supply were turned off, the samples were cooled down to room temperature in 4 hrs approximately.

The films surface morphology was analyzed by scanning electron microscopy (SEM) and atomic force microscopy (AFM) in non-contact mode. X-ray diffraction (XRD) using a Cu Ka radiation source was used to evaluate the films crystalline structure. The structural properties were also studied by micro Raman scattering (RS) using the 632.8nm line of a He–Ne laser with a power of 20mW.

3. Results and Discussion

In order to calculate the films thickness (FT), we employed a mask on the substrates to produce ***in- situ*** a step on the GaMnAs film during growth. The films thickness was about 0.1 μm and it was obtained from depth profile on step measured by a KLA- long scan surface profiler in a 214 μm length and 50 μm/s speed, as indicating in the Fig. 1. We did not observe changes in the films thickness with growth temperature.

In the Figure 2 (lef column), we show SEM images (with a magnification of x 10000) taken in plan view on the samples grown at (a) 400 ^oC, (b) 500 ^oC, and (c) 520 ^oC. The SEM images show that the surface is flat, but the samples b) and c) show small particles scattered over the surface. The Mn concentration was obtained from energy dispersive spectroscopy (EDS). AFM images were taken to analyze details of the film surface morphology. In the right column of Fig. 2, we show AFM images in a $1x1\mu m^2$ scale.

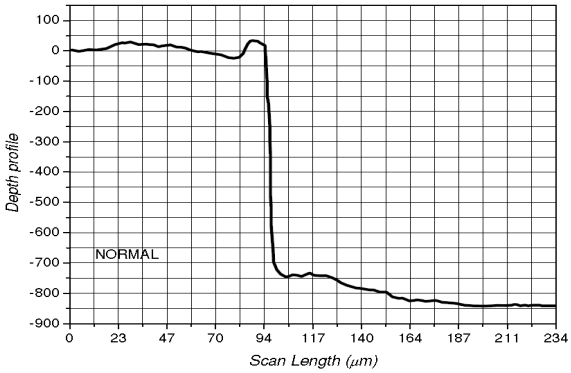

Fig. 1: Depth profile taken by using a profiler on a step made in situ in a GaAsMn sample.

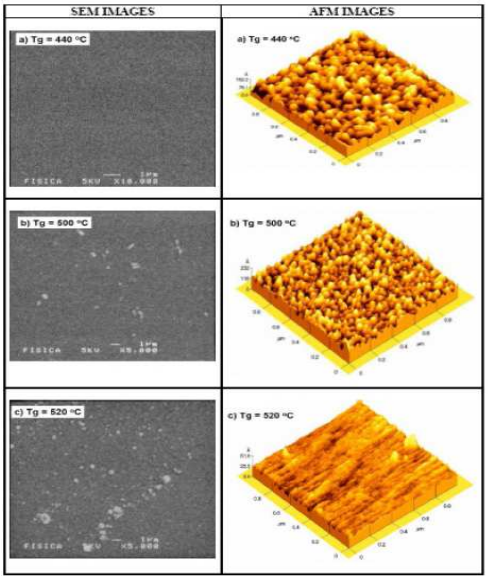

Fig. 2: Plan view SEM images (left) taken with a magnification of x10000, and AFM images (right) taken in a 1x1 μm^2 area of $Ga_{1-x}AsMn_x$ samples grown at: a) Tg = 400 ^oC (x=0.04), b) Tg = 500 ^oC (x=0.24) c) Tg = 520 ^oC (x=0.28).

The AFM images show that the films are composed of grains with size in the order of 100 nm. From these images we observe that the grains are approximately oval shaped, and their size tends to decrease with growth temperature. The RMS surface roughness values obtained from the AFM measurements are: a) 15.7 Å, b) 17.7 Å and c) 2.45 Å, respectively.

X-ray diffractions of the $Ga_{1-x}AsMn_x$ samples were performed with θ-2θ scans and step size 2θ = 0.02 ° at room temperature by using Cu K_α radiation. Fig. 3 d) is the XRD curve of the GaAs (x=0) sample grown at Tg = 500 °C taken as reference. In this spectra only appear the (002) and (004) substrate main peaks, and suggest that the XRD curve is dominated by the substrate characteristics. For the $Ga_{1-x}AsMn_x$ samples grown at: a) Tg = 400 °C (Mn=5%), b) Tg = 500 °C (Mn=24%), and c) Tg = 520 °C (Mn=28%); additional to the GaAs main peak appeared more peaks not well defined such as (220) and others (labeled by (+) in the Fig. 1 d)) corresponding possibly to α-Mn phase, and Ga_5Mn_8 [8], respectively.

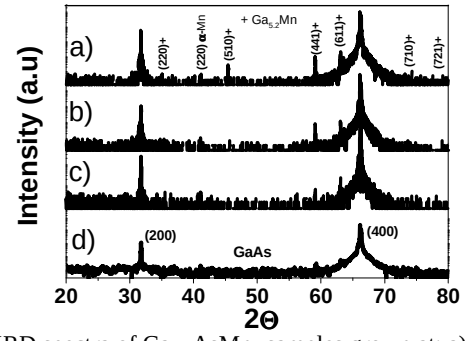

Fig. 3: XRD spectra of $Ga_{1-x}AsMn_x$ samples grown at: a) Tg = 400 °C (x=0.05), b) Tg = 500 °C (x=0.24), c) Tg = 520 °C (x=0.28) and d) Tg = 500°C (x=0.0) taken as a reference. The peaks labeled as (+) in this Fig. beyond to the $Ga_{0.5}Mn$ phase.

The crystal structure of α-Mn is FCC with lattice constant a = 0.89121 nm. It is observed that some peaks of the samples b) and c) tend to increase their intensities by increasing the substrate temperature and/or the Mn content, probably due to an enhancement of the phase segregation or enhancement of Mn_mAs_n cluster formation as suggest the Raman spectra that will discuses below [9]. A more detail analysis (not shown here) realized on the surface of the samples by using grazing angle X-ray diffraction show that the samples have a very poor crystalline quality.

Now, we analyze the Raman spectra for structural properties. Fig. 4 shows the Raman spectra of $Ga_{1-x}AsMn_x$ films taken in backscattering configuration z´(x´, x´)-z´. In order to obtain a very short penetration depth, and avoiding any Raman scattering from the substrate we used the 632.8 nm line from a He-Ne laser as an excitation light source. For comparison in the Fig. 4 d) we included the Raman spectra of a GaAs (x=0) sample grown at identical substrate temperature of the sample b). According to the Raman selection rules for a zinc blenda crystal, the LO mode is allowed, but TO mode is forbidden in this configuration. A weak signal observed in 266 cm^{-1} (TO mode), is attributed to structural disorder in the GaAs matrix. Additional peak located at 532 cm^{-1} is the 2TO(Γ) resonant second phonon mode [10]. This mode presents a redshift of 2 cm^{-1} probably due to lattice mismatch stress and alloy effects.

In all Raman spectra for the samples grown at substrate temperatures between 440°C ≤ Tg ≤ 520°C, the intensity of the LO Raman mode decreases dramatically probably by the incorporation of Mn atoms in the GaAs matrix. Near to LO_{GaAs}, in 263 cm^{-1}, a weak coupled-LO-phonon plasmon mode (CLOPM) is also observed [11]. This mode appears by the lattice disorder and other built-in defects induced when more Mn atoms are incorporating in the GaAs matrix. On the other hand, disorder acoustic longitudinal actived (DALA) modes in the range of 178 cm^{-1} to 270 cm^{-1} were observed. Similar results have been observed in Mn ion-implanted GaAs [12].

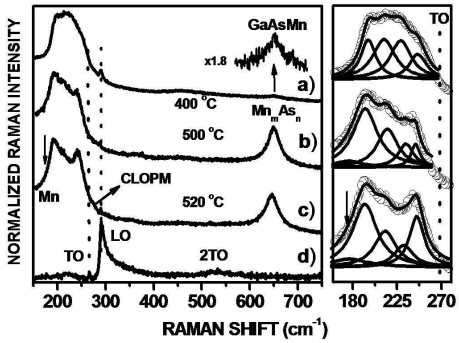

Fig. 4: Room temperature Raman spectra (left) of $Ga_{1-x}AsMn_x$ samples grown at: a) Tg = 400 °C (x=0.05), b) Tg = 500 °C (x=0.24), c) Tg = 520 °C (x=0.28), and d) Tg = 500 °C (x=0.0) taken as a reference. Deconvolution of the $Ga_{1-x}AsMn_x$ Raman spectra experimental data (right) by using six Gaussian functions. The arrows indicate the position of Mn and As modes.

In order to locate the exact peak positions, we obtained the best fitting by using three Lorentzian functions as indicating in the right side on Fig. 4. It is found that the peaks located at 172.6 cm^{-1} and 234.2 cm^{-1} are related to Mn and As vibrational modes (labeled by arrows in the Figure) for the all samples with have high Mn concentration. For the samples a) the As peak is dominant due to the lower Mn content. Additional peaks located at 192.2, 212.6, and 244.5 cm^{-1} are probably associated with vacancy-related defects, such as V_{Ga} vacancies or Mn_{Ga} complex.

Besides, a new phonon mode centered on 648±2 cm^{-1} is observed for the all samples with high Mn content. This peak can be assigned to a disorder activated Raman on the border of the Brillouin zone (BZ), corresponding to the acoustic and optical phonon branches due to the incorpora-

tion of Mn-As pairs or Mn_mAs_n cluster formation in the GaAs matrix. Similar results have been reported in layers of GaN implanted with Mn [13]. As far as we know this is the first report of the frequency Raman position of Mn_mAs_n complex in this material. In order to theoretical estimate the frequency of this Raman mode, we used the mass reduced model given by the following equation [14]:

$$\omega_{(Mn)m-(As)n} \approx \omega_{2LOGa-As}\sqrt{\frac{\mu_{Ga-As}}{\mu_{(Mn)m-(As)n}}} \quad (1)$$

Where $\omega_{2LOGa-As}$ is the frequency of phonon E_1(TO) and μ_{Ga-As}, $\mu_{(Mn)m-(As)n}$ are the reduced masses of the $Ga-As$ and $(Mn)_m-(As)_n$ pairs , respectively.

Table No. 1. Theoretical calculation of the Raman frecuencies by using the mass reduced model.

m	n	$\omega_{(Mn)m-(As)n}$
2	1	555
3	2	626
4	4	650
4	3	641
4	2	603
5	4	648
5	3	634
5	2	510

The Raman frequencies calculated for us using the Eq. (1), are showing in the table 1. The ω_{ASMn} = 650 cm^{-1}, correspondin to *l*=2 and *k* = 4, is in good agreement with the experimental value centered at 650 cm^{-1} for sample a) (Mn =5%), 648.7 cm^{-1} b) (Mn =24%) and 645.2 cm^{-1} for the sample c) (Mn=28%). The ω_{ASMn} Raman mode present a blue-shift depending of Mn concentration. The formation of $(GaAs)_nMn_m$ complex has been predicted theoretically by G.L. Gutsev, *et al* [15]. Clusters are likely formed by MnAs units because the pure Mn_m clusters possess the antiferromagnetic coupling of local excess spin densities, that drastically reduces the cluster magnetic moments [16,17]. The study of cluster formations is interesting, because the clustering of Mn atoms inside the GaAs host is a possible path toward increasing the Curie temperature (Tc) important to technological applications in spintronics.

4. Conclusion

We have studied the properties of $Ga_{1-x}Mn_xAs$ films grown by RF magnetron sputtering. X-ray diffractions show that the samples have a poor crystalline quality. The Raman peaks located at 192.2, 212.6, and 244.5 cm^{-1} are possibly due to defects related to the Mn content. By using the mass reduced model we found the Raman frequency at 650 cm^{-1}, in good agreement with the experimental data. This peak is related to a disorder Raman activated due to Mn_mAs_n cluster formation on GaAs host.

5. Acknowledgments

This work was partially supported by **DIMA -** Proyect "*Propiedades Magneto- Ópticas de Aleaciones Semiconductoras de GaAsMn Crecidas por MBE y Magnetrón Sputtering"*. Código 20201004926, and CONACYT-Mexico. The authors thank the technical assistance of A. Sotelo, R. Fragoso, A. Soto and E. Gomez.

References

[1] N. Samarth, S.H. Chun1, K.C. Ku, S.J. Potashnik, P. Schiffer. Solid State Communications 127 (2003) 173.

[2] J. De Boeck, R. Oesterholt, A. Van Hesch, H. Bender, C. Bruynseraede, C. Van Hoof, G. Borghs, Appl. Phys. Lett. 2744 (1996) 68.

[3] F. Matsukura, H. Ohno, A. Shen, Y. Sugawara, Phys. Rev. B 57 (1998) R2037.

[4] A. Shen, F. Matsukura, S.P. Guo, Y. Sugawara, H. Ohno, M. Tani, H. Abe, Liu, J. Cryst. Growth 201/202 (1999) 679.

[5] M. Tanaka, J.P. Harbison, J. DeBoeck, Appl. Phys. Lett. 62 (1993) 1565.

[6] K.H. Kim, J.H. Park, B.D. Kim, C.S. Kim, D. Kim, H.J. Kim, Y.E. Ihm, Met. Mater. 8 (2002) 177.

[7] A. Shen, F. Matsukura, S.P. Guo, Y. Sugawara, H. Ohno, M. Tani, H. Abe, Liu, J. Cryst. Growth 201/202 (1999) 679.

[8] H. Ohno, F. Matsukura, T. Omia, N. Akida, J. Appl. Phys. 81 (1999) 4277.

[9] A. Shen, F. Matsukura, S.P. Guo, Y. Sugawara, H. Ohno, M. Tani, H. Abe, Liu, J. Crystal Growth 201/202 (1999) 679.

[10] A. Pulzara Mora. Ph.D Thesis. Cinvestav, Mexico D.F, 2006.

[11] M.R. Slam, N.F. Chen, M. Materials Science in Semiconductor Processing. Vol. 9, (2006) 184.

[12] Sauncy T, Holtz M, Zallen R. Phys Rev B. 50 (1994) 10702.

[13] Y.H. Zhang, L.L. Guo, W.Z. Shen. Materials Science and Engineering B 130 (2006) 269.

[14] X. Yang, J Wu, Z. Chen, Y. Pan, Y. Zhang, Z. Yang, T. Yu, G. Zhang. Solid State Communications 143 (2007) 236.

[15] G.L. Gutsev, M.D. Mochena, C.W. Bauschlicher Jr. Chemical Physics Letters 439 (2007) 95.

[16] Th. Hartmann et al., Physica E 13 (2002) 572.

[17]G.L. Gutsev, M.D. Mochena, C.W. Bauschlicher Jr., J. Phys. Chem. A 110 (2006) 9758.